Notes on solving Maxwell equations, part I, finite elements method using vector elements

EINDHOVEN UNIVERSITY OF TECHNOLOGY
Department of Mathematics and Computer Science

CASA-Report 11-10
February 2011

Notes on solving Maxwell equations Part 1: Finite elements method using vector elements

by

R. Rook

Centre for Analysis, Scientific computing and Applications
Department of Mathematics and Computer Science
Eindhoven University of Technology
P.O. Box 513
5600 MB Eindhoven, The Netherlands
ISSN: 0926-4507

Notes on solving Maxwell equations Part 1: Finite Elements Method using vector elements

R.Rook

February 3, 2011

1 Introduction

The content of this document is a brief description of the steps taken in the process of designing and writing a simulation program for solving the Maxwell equations using the finite element method (FEM). It covers the theory from the literature by various authors. It deals with the conversion to certain conventions, like the orientation of axis and the time convention for time-harmonic solutions and the non-dimensionalization process. The mathematical foundation is far from complete, but the reader is referred to the literature for the details.

The application is the scattering by an object of electromagnetic waves. Part 2 will cover the far-field calculation given the near-field solution obtained by the FEM.

2 Problem

A typical problem is an incident plane wave refracting and diffracting by a 2D-periodic object (e.g. a resist line in air on top of a layered substrate, see figure 1). The Maxwell equations with the proper boundary conditions are the governing equations.

The materials are assumed to be isotropic and homogeneous within the materials (constant permittivity and permeability).

2.1 Maxwell Equations

The time convention used in this report is $\exp(-i\omega t)$ (as used by the authors Chew, Monk), where angular frequency ω [s^{-1}], $\omega > 0$. This particular choice results the intuitive case that waves with a certain wave number travel in the

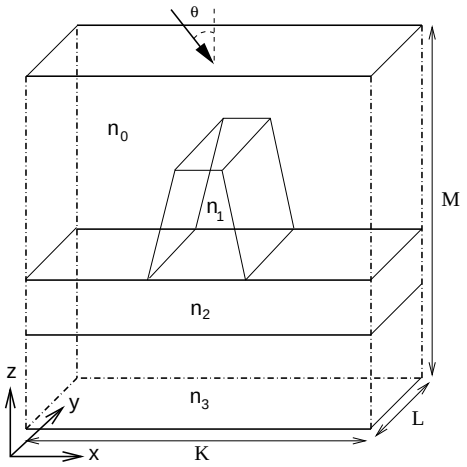

Figure 1: 2D-grating on Ω

corresponding direction of the axis, e.g. $\exp(ikx - i\omega t)$, with $k > 0$, travel in the positive x-direction. Note that converting a solution, say E, to the $\exp(i\omega t)$ time convention (as used by the author Zhu & Cangellaris) is simply the conjugated solution $\bar{E}$.

2.1.1 Dimensional

On a domain $\Omega \in R^3$, the time-harmonic electric field E [Vm^{-1}], the time-harmonic magnetic field H [Am^{-1}], electric displacement D [Cm^{-2}] and magnetic induction B [T] for isotropic linear media are described by

(Faraday's law)

$$\nabla \times E = i\omega B - M$$

(Ampère's law)

$$\nabla \times H = J - i\omega D,$$

(Ohm's law)

$$J = J_c + J_v,$$

(Gauss' electric field law)

$$\nabla \cdot D = \frac{1}{i\omega} \nabla \cdot J$$

(Gauss' magnetic field law)

$$\nabla \cdot B = \frac{1}{i\omega} \nabla \cdot M,$$

with the complex electric permittivities ϵ [Fm^{-1}] and permeability μ [Hm^{-1}]. The electric current density J_v [Am^{-2}] represents the impressed current sources in the domain (imposed electric field), J_c [Am^{-2}] accounts for induced current flow in the medium due to the rpecence pf conductor and/or dielectric loss and M [Ts^{-1}] is the non-physical magnetic current density source.

The constitutive relations between the electromagnetic field quantities and theit associated flux densities for isotropic materials are given by

$$D = \epsilon E,\ B = \mu H,\ J_c = \gamma E,$$

with γ [Sm^{-1}] is the (scalar) conductivity.

Then, in each isotropic material, the vector wave Maxwell equations can be derived as

$$\nabla \times (\nabla \times E) - k^2 E = i\omega\mu J - \nabla \times M,$$

$$\nabla \times (\nabla \times H) - k^2 H = i\omega\epsilon M + \nabla \times J,$$

with $k^2 = \omega^2 \mu\epsilon$ and shows the symmetry between the electric and magnetic fields (the duality principle; Chew, page 9).

If the effective permittivity is $\tilde{\epsilon} = \epsilon - i\gamma/\omega$, a material with index i has the (effective) relative refraction index $n_i^2 = \mu\tilde{\epsilon}/\mu_0\epsilon_0 = \mu_{r,i}\epsilon_{r,i}$, where $\mu_{r,i}$ [-] and $\epsilon_{r,i}$ [-] are the relative permittivity and permeability, respectively. In air at low field strengths (same as in vacuum $\gamma = 0$, $\epsilon = \epsilon_0$, $\mu = \mu_0$), the reference wave number k_0 [m^{-1}] is defined as $k_0^2 = \omega^2\mu_0\epsilon_0 = \omega^2/c^2$, with c the speed of light in vacuum. Combining these with the relation for the wave length in air $\lambda_0 = 2\pi n_0/k_0$ [m], we can derive an expression for the frequency squared wave number for the i-th material $k_i^2 = \omega^2\mu\tilde{\epsilon} = 4\pi^2 n_i^2/\lambda_0^2$ or $k_i = k_0\, n_i/n_0$.

From these relations (and zero magnetic current density M), we derive the time-harmonic vector wave Maxwell equation (Zhu & Cangellaris, page 15; Monk, page 7)

$$\nabla \times (\nabla \times E) - k_i^2 E = i\omega\mu J_v.$$

2.1.2 Non-dimensional

Spatial variables x, y and z are non-dimensionalized with respect to wave length λ_0 as the used wavelengths are comparable to the dimensions of the scatterer. The domain is reduced to a rectangular domain $\Omega = [0, K] \times [0, L] \times [0, M]$, with finite K, L and M [m] in each direction.

The unknowns are the non-dimensional electric vector field $E(x, y, z)$ and the magnetic vector field $H(x, y, z)$, where E_0 is a reference value, e.g. the amplitude of the incident field. Take $H_0 = \sqrt{\frac{\epsilon_0}{\mu_0}} E_0$ as reference value (intrinsic impedance in free space) for the magnetic field and $J_{v0} = H_0/\lambda_0$ for the current density source and $M_0 = E_0/\lambda_0$ for the magnetic current density.

After non-dimensionalization, the field relations are

$$H = \frac{1}{2\pi i n_0 \mu_{r,i}} (\nabla \times E + M), \tag{1}$$

and

$$E = \frac{1}{2\pi i n_0 \epsilon_{r,i}} (J_v - \nabla \times H), \tag{2}$$

where we used $\omega \tilde{\epsilon} \sqrt{\frac{\mu_0}{\epsilon_0}} \lambda_0 = \omega \epsilon_{r,i} \epsilon_0 \sqrt{\frac{\mu_0}{\epsilon_0}} \lambda_0 = \omega \epsilon_{r,i} \sqrt{\epsilon_0 \mu_0} \lambda_0 = \epsilon_{r,i} k_0 \lambda_0 = 2\pi n_0 \epsilon_{r,i}$. The electric field E will satisfy the following (non-dimensional) Maxwell equation (from now on the refraction index for air $n_0 = 1$)

$$\nabla \times (\nabla \times E) - 4\pi^2 n_i^2 E = 2\pi i \mu_{r,i} J_v.$$

Instead of the full field E we can rewrite the problem for the scattered field

$$E^{\text{scat}} = E - E^{\text{inc}},$$

with E^{inc} a solution in air ($i = 0$). So, the scattered field satisfies (no current sources, $J_v = 0$)

$$\nabla \times (\nabla \times E^{\text{scat}}) - 4\pi^2 n_i^2 E^{\text{scat}} = 4\pi^2 (n_i^2 - n_0^2) E^{\text{inc}},$$

which is referred to as the scattered field formulation, where materials (other than air) will act as sources.

Another description is the contrast formulation for the grating problem

$$E^{\text{contr}} = E - E^{\text{multi}},$$

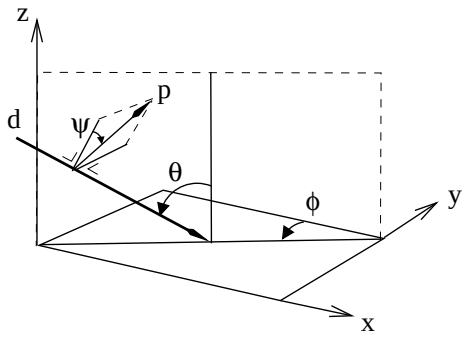

Figure 2: Conical incident wave

where E^{inc} is replaced by the exact solution of the multiple layer stack E^{multi} (thus without the grating). In this case E^{contr} satisfies

$$\nabla \times (\nabla \times E^{\text{contr}}) - 4\pi^2 n_i^2 E^{\text{contr}} = 4\pi^2 (n_i^2 - n_{\text{res}}^2) E^{\text{multi}},$$

where $n_{\text{res}} = n_0$ in and $n_{\text{res}} = n_i$ outside the scatterer, which makes the right-hand side is non-zero in the resistor only.

2.1.3 Scalar wave equations and polarization

In an isotropic medium where the electromagnetic properties are varying in one direction, say the z-direction, the Maxwell equations can be reduced to two scalar equations that are decoupled. They characterize two types of waves: the transverse-electric (TE_z or TE) and the transverse-magnetic (TM_z or TM) waves. Assuming that the field is linearly polarized, the electric field in the TE waves are directed in the x, y-plane and can be rotated around the z-axis to point only in the y-direction $E = E_y$. A better way of characterizing this wave is to use the z-component of the magnetic field H_z. If $H_z \neq 0$, the field describe TE waves. Similarly, by duality, the E_z component characterizes TM waves (Chew, page 45).

2.1.4 Incident wave

The general incident (polarized) wave in air is

$$E^{\text{inc}} = p \exp(2\pi i n_0 d \cdot x),\ p \cdot d = 0.$$

For a conical incident wave, the vector p is the unit vector

$$p = \begin{bmatrix} \cos(\psi)\cos(\theta)\cos(\phi) - \sin(\psi)\sin(\phi) \\ \cos(\psi)\cos(\theta)\sin(\phi) + \sin(\psi)\cos(\phi) \\ \cos(\psi)\sin(\theta) \end{bmatrix},$$

where ψ is the polarization angle ($\pi/2$ for TE and 0 for TM), θ is the polar angle and ϕ is the azimuth of the incident wave. It is perpendicular to the wave direction d

$$d = \begin{bmatrix} \sin(\theta)\cos(\phi) \\ \sin(\theta)\sin(\phi) \\ -\cos(\theta) \end{bmatrix}.$$

2.2 Boundary conditions

In general, two types of boundary conditions are specified: Robin type Silver-Müller condition (Monk, page 11) and (essential) Dirichlet boundary conditions or PEC boundaries (Monk, page 9; Zhu & Cangellaris, page 6).

2.2.1 Silver-Müller

On the outside boundary we may pose the Silver-Müller condition as a Robin type condition

$$n \times (\nabla \times E) - \sigma E_T = -r, \tag{3}$$

with

$$r = -n \times (\nabla \times E^{\text{inc}}) + \sigma E_T^{\text{inc}},$$

and where $E_T = n \times (E \times n)$, the tangential projection of E on the boundary surface. Note that in the scattered field or contrast field formulation, the right-hand side vanishes $r = 0$ and the Silver-Müller condition reduces to a homogeneous condition.

2.2.2 Dirichlet

When the solution is known, we may pose Dirichlet or essential boundary conditions

$$E = E^{\text{inc}}(x).$$

Note that the tangential part of the incident wave only contributes to the problem.

2.2.3 Perfectly conducting

At perfect electrically conduction (PEC) boundaries $n \times E = 0$ holds, with n the normal direction of the boundary.

2.2.4 Periodic boundaries

The quasi-periodic boundary conditions are defined as

$$E(K, y, z) = E(0, y, z) \exp(2\pi i n_0 K d_1),$$

$$E(x, L, z) = E(x, 0, z) \exp(2\pi i n_0 L d_2),$$

$$E(x, y, M) = E(x, y, 0) \exp(2\pi i n_0 M d_3)$$

in the x-, y- and z-direction, respectively.

3 Finite Element Method

As the geometry involves arbitrary shapes, the problem is solved using FEM with vector basis functions. The FEM allows us to create a mesh consisting of triangular elements that perfectly overlays the geometry. The vector functions solve a number of problems surfacing when using standard node-based scalar base functions: the problem of spurious modes. The first is the enforcement of the tangential electric and magnetic field continuity at the material interfaces. Also the continuity of the normal components of the electric and magnetic flux densities cannot be guaranteed. The second is the inability to model properly the null space of the curl operator (the null space consist of all vector fields $F = -\nabla\Psi$, where Ψ is an arbitrary scalar field) (Zhu & Cangellaris, page 15).

3.1 Variational formulation

In the Galerkin method, this solution satisfies the variational formulation

$$\int_\Omega (\nabla \times E) \cdot (\nabla \times \phi) - 4\pi^2 n_i^2 E\phi dV + \oint n \times (\nabla \times E)\phi_T d\Gamma = \int_\Omega F\phi dV$$

or when the Robin boundary condition (3) is included

$$\int_\Omega (\nabla \times E) \cdot (\nabla \times \phi) - 4\pi^2 n_i^2 E\phi dV + \oint \sigma E_T \phi_T d\Gamma = \int_\Omega F\phi dV + \oint r\phi_T d\Gamma, \quad (4)$$

for all $\phi \in H(\mathrm{curl}; \Omega)$.

The Dirichlet boundary conditions have the following variational form

$$\oint E_T \phi_T d\Gamma = \oint r\phi_T d\Gamma.$$

Note that within the variational formulation (4), if you set σ and r to a large value, say 10^{10}, you obtain a the same result (within a certain accuracy). This is also known as the penalty method, but this will destroy a well-conditioned mass matrix. Rather eliminate the Dirichlet boundary condition from the system of equations.

Assume that the perfectly conducting boundary conditions are located on Γ and the Silver-Müller conditions on Σ. In order for all the integrals to be well-defined, we should use the space X defined by

$$X = \left\{ u \in H(\mathrm{curl}; \Omega) \mid n \times u = 0 \text{ on } \Gamma \wedge u_T \in (L^2(\Sigma))^3 \text{ on } \Sigma \right\}$$

with the Sobolev space

$$H(\mathrm{curl}; \Omega) = \left\{ v \in (L^2(\Omega))^3 \mid \nabla \times v \in (L^2(\Omega))^3 \right\}.$$

However, note that X is not ideal to define the finite elements space on (Monk, page 99) as it contains the null-space for the curl operator.

3.2 Affine maps

A finite element is defined by the triple (K, P_K, Σ_K), where K is a geometric domain, P_K is the space of functions on K and Σ_K a set of functionals on P_K also called the degrees of freedom (DOFs) of the finite element. An important step is to map a these elements to a reference element $(\hat{K}, P_{\hat{K}}, \Sigma_{\hat{K}})$.

The solution E is approximated and will be the sum of the shape functions ϕ_i:

$$E = \sum L_i(E)\phi_i,$$

where L_i are the DOFs in the system.

Suppose the domain is subdivided into elements K. We can define the shape functions on these elements. These shape functions are mapped with an iso-parametric mapping $F_K : \hat{x} \to x$ from reference element $\hat{K}$ to the physical element K. For tetrahedra we take the affine mapping of the 4 vertices. The functions and their derivatives in the variational formulation are then transformed in the following way

$$(\nabla \times \phi) \circ F_K = \frac{1}{\det(\mathrm{d}F_K)} \mathrm{d}F_K \hat{\nabla} \times \hat{\phi}$$

$$\phi \circ F_K = (\mathrm{d}F_K)^{-T} \hat{\phi}$$

The (affine) mapping F_K is constant on K and we have $\hat{E} = \sum \hat{L}_i(\hat{E})\hat{\phi}_i$, thus $\hat{L}_i = L_i$. This means that the sets of DOFs on K are invariant under transformation (see Monk, Lemma 5.34, page 131). The vector elements described below are formulated on these reference elements.

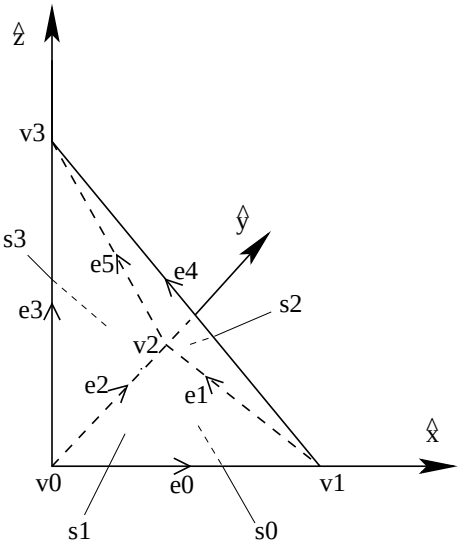

(a) Local numbering vertices and DOFs

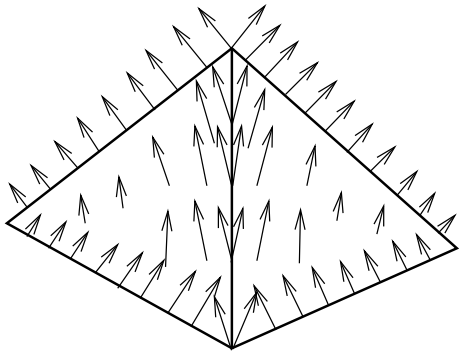
(b) Basis function

3.3 Curl-conforming elements

Curl-conforming means that the finite element space that is a subspace of $H(\text{curl};\Omega)$. The first family of curl-conforming elements (edge elements) has shape functions that span the polynomial space $R_k = (P_{k-1})^3 \oplus S_k$, with $S_k = \{p \in (\tilde{P}_k)^3 \mid x \cdot p = 0\}$, P_k the space of polynomial functions with order $k \geq 1$ and $\tilde{P}_k$ the set of homogeneous polymials with exact order k (Monk, page 108). A second family of curl-conforming elements can be obtained, where the space of functions is larger $P_K = (P_k)^3$, e.g. *hp*-elements (Monk, page 202; Pavel). This family of elements is not part of this report.

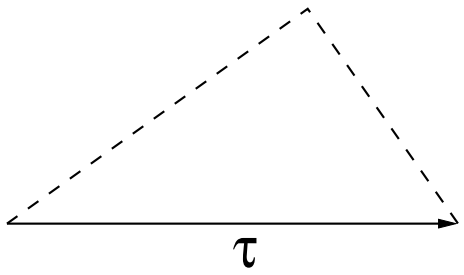

Figure 3: Definition edge tangential

3.3.1 Whitney element

The Whitney element, or linear edge element is the lowest order curl-conforming element and resolves space R_1.

The degree of freedom L_j is defined on the j-th edge in the mesh, and is the integral of the inner product of the solution and the tangential vector τ_{e_j} defining that edge:

$$L_j(E) = \frac{1}{\text{length}(e_j)} \int_{e_j} \tau_{e_j} \cdot E \, ds.$$

In Whitney elements, the shape functions are constructed from the barycentric coordinates

$$\lambda_0 = 1 - \hat{x} - \hat{y} - \hat{z},$$

$$\lambda_1 = \hat{x},\ \lambda_2 = \hat{y},\ \lambda_3 = \hat{z},$$

and the shape functions are derived by

$$\hat{\phi}_{e\{i,j\}} = \lambda_i \hat{\nabla} \lambda_j - \lambda_j \hat{\nabla} \lambda_i,$$

where $e\{i,j\}$ is the edge with vertices i and j $(i,j = 0,...,3)$, on which the shape function is defined.

This results in the following set of $k = 6$ shape functions:

$$\begin{array}{ll}
\hat{\phi}_0 = \hat{\phi}_{e\{0,1\}} = & [1 - \hat{y} - \hat{z}, \hat{x}, \hat{x}]^T \\
\hat{\phi}_1 = \hat{\phi}_{e\{1,2\}} = & [-\hat{y}, \hat{x}, 0]^T \\
\hat{\phi}_2 = \hat{\phi}_{e\{0,2\}} = & [\hat{y}, 1 - \hat{x} - \hat{z}, \hat{y}]^T \\
\hat{\phi}_3 = \hat{\phi}_{e\{0,3\}} = & [\hat{z}, \hat{z}, 1 - \hat{x} - \hat{y}]^T \\
\hat{\phi}_4 = \hat{\phi}_{e\{1,3\}} = & [-\hat{z}, 0, \hat{x}]^T \\
\hat{\phi}_5 = \hat{\phi}_{e\{2,3\}} = & [0, -\hat{z}, \hat{y}]^T
\end{array}$$

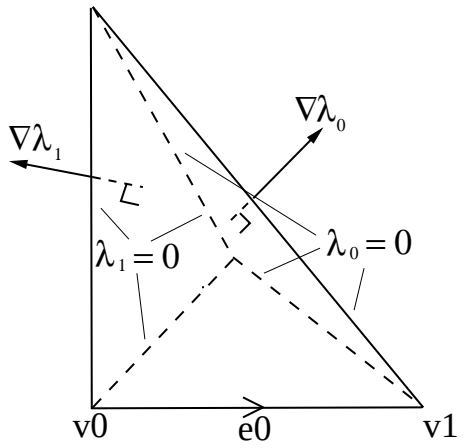

Figure 4: Barycentric coordinates

and their curls

$$\hat{\nabla} \times \hat{\phi}_0 = [0, -2, 2]^T, \hat{\nabla} \times \hat{\phi}_1 = [0, 0, 2]^T$$

$$\hat{\nabla} \times \hat{\phi}_2 = [2, 0, -2]^T, \hat{\nabla} \times \hat{\phi}_3 = [-2, 2, 0]^T$$

$$\hat{\nabla} \times \hat{\phi}_4 = [0, -2, 0]^T, \hat{\nabla} \times \hat{\phi}_5 = [2, 0, 0]^T$$

These functions are defined in the reference space $\hat{K}$.

3.3.2 Quadratic edge elements

R_2 is spanned by 20 polynomial vectors. The first 12 spans the space $(P_1)^3$ and are the Whitney shape functions with 6 additional linear shape functions which related to the DOFs

$$L'_j(E) = \frac{1}{\text{length}(e_j)} \int_{e_j} E \cdot \tau_{e_j}(3 - 6s)\, ds.$$

The other 8 shape functions are related to the faces and their DOFs are

$$L_j(E) = \frac{1}{\text{area}(f_j)} \int_{f_j} E \cdot (-8\tau_{1j} + 4\tau_{2j})\, dA$$

and

$$L'_j(E) = \frac{1}{\text{area}(f_j)} \int_{f_j} E \cdot (4\tau_{1j} + 4\tau_{2j})\, dA$$

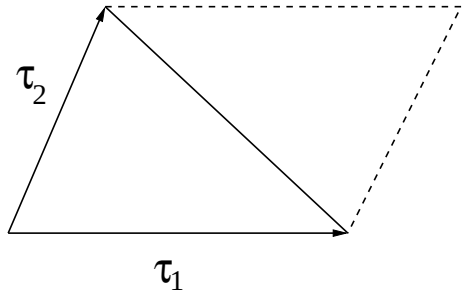

Figure 5: Definition face tangentials

where $\tau_{1j}$and τ_{2j} span the 2 sides of the triangular face. Note that area$(f_j) = \frac{1}{2}\left\|\tau_{1j} \times \tau_{2j}\right\|$.

The shape functions are the 6 Whitney shape functions from the previous section and 6 additional linear edge functions

$$\hat{\phi}'_{e\{i,j\}} = \lambda_i \hat{\nabla}\lambda_j + \lambda_j \hat{\nabla}\lambda_i,$$

or

$$\begin{aligned}
\hat{\phi}_6 = \hat{\phi}'_{e\{0,1\}} = &\quad [1 - 2\hat{x} - \hat{y} - \hat{z}, -\hat{x}, -\hat{x}]^T \\
\hat{\phi}_7 = \hat{\phi}'_{e\{1,2\}} = &\quad [\hat{y}, \hat{x}, 0]^T \\
\hat{\phi}_8 = \hat{\phi}'_{e\{0,2\}} = &\quad [-\hat{y}, 1 - \hat{x} - 2\hat{y} - \hat{z}, -\hat{y}]^T \\
\hat{\phi}_9 = \hat{\phi}'_{e\{0,3\}} = &\quad [-\hat{z}, -\hat{z}, 1 - \hat{x} - \hat{y} - 2\hat{z}]^T \\
\hat{\phi}_{10} = \hat{\phi}'_{e\{1,3\}} = &\quad [\hat{z}, 0, \hat{x}]^T \\
\hat{\phi}_{11} = \hat{\phi}'_{e\{2,3\}} = &\quad [0, \hat{z}, \hat{y}]^T
\end{aligned}$$

These result in 2 functions per edge.

The other 8 functions spans S_2 and have the form

$$\hat{\phi}_{s\{i,j,k\}} = \lambda_i \lambda_j \hat{\nabla}\lambda_k - \lambda_i \lambda_k \hat{\nabla}\lambda_j$$

and

$$\hat{\phi}'_{s\{i,j,k\}} = \lambda_i \lambda_j \hat{\nabla}\lambda_k - \lambda_j \lambda_k \hat{\nabla}\lambda_i$$

These are related to the faces (also 2 functions per face):

$$
\begin{aligned}
\hat{\phi}_{12} = \hat{\phi}_{s\{0,1,2\}} &= [-(1-\hat{x}-\hat{y}-\hat{z})\hat{y}, (1-\hat{x}-\hat{y}-\hat{z})\hat{x}, 0]^T \\
\hat{\phi}_{13} = \hat{\phi}'_{s\{0,1,2\}} &= [\hat{x}\hat{y}, (1-\hat{x}-\hat{z})\hat{x}, \hat{x}\hat{y}]^T \\
\hat{\phi}_{14} = \hat{\phi}_{s\{0,1,3\}} &= [-(1-\hat{x}-\hat{y}-\hat{z})\hat{z}, 0, (1-\hat{x}-\hat{y}-\hat{z})\hat{x}]^T \\
\hat{\phi}_{15} = \hat{\phi}'_{s\{0,1,3\}} &= [\hat{x}\hat{z}, \hat{x}\hat{z}, (1-\hat{x}-\hat{y})\hat{x}]^T \\
\hat{\phi}_{16} = \hat{\phi}_{s\{1,2,3\}} &= [0, -\hat{x}\hat{z}, \hat{x}\hat{y}]^T \\
\hat{\phi}_{17} = \hat{\phi}'_{s\{1,2,3\}} &= [-\hat{y}\hat{z}, 0, \hat{x}\hat{y}]^T \\
\hat{\phi}_{18} = \hat{\phi}_{s\{0,2,3\}} &= [0, -(1-\hat{x}-\hat{y}-\hat{z})\hat{z}, (1-\hat{x}-\hat{y}-\hat{z})\hat{y}]^T \\
\hat{\phi}_{19} = \hat{\phi}'_{s\{0,2,3\}} &= [\hat{y}\hat{z}, \hat{y}\hat{z}, (1-\hat{x}-\hat{y})\hat{y}]^T
\end{aligned}
$$

In general, the shape functions ϕ_j do not form a set of functions with the δ-property, with respect to the linear forms L_i (DOFs). However, we can construct one. Suppose we have our basis $\{\phi_j\}$ and we are looking for another basis $\{\theta_j\}$ such that

$$\theta_j = \sum_{k=1}^{N} a_{kj}\phi_k.$$

So,

$$L_i(\theta_j) = L_i\left(\sum_{k=1}^{N} a_{kj}\phi_k\right) = \sum_{k=1}^{N} a_{kj}L_i(\phi_k) = \delta_{ij}$$

which reduces to $LA = I$, with $L = \{L_i(\phi_k)\}_{i,k=1}^{N}$. For each element p in the polynomial space we have

$$p = \sum_j L_j(p)\theta_j = \sum_j L_j(p)\sum_k a_{kj}\phi_k = \sum_k\sum_j a_{kj}L_j(p)\phi_k = \sum_k c_k(p)\phi_k$$

with

$$c_k(p) = \sum_j a_{kj}L_j(p),$$

the DOFs corresponding to the basis $\{\phi_k\}$.

The resulting matrix A for the second order Nedelec finite element is

$$A = \begin{bmatrix} I & 0 \\ -B & I \end{bmatrix},\ B = \{L_i(\phi_j)\}_{i=12,19}^{j=0,11}$$

and explicitly,

$$B = \begin{bmatrix}
-4 & 4 & 0 & 0 & 0 & 0 & -1\tfrac{1}{3} & -1\tfrac{1}{3} & 2\tfrac{2}{3} & 0 & 0 & 0 \\
4 & 0 & 4 & 0 & 0 & 0 & -1\tfrac{1}{3} & 2\tfrac{2}{3} & -1\tfrac{1}{3} & 0 & 0 & 0 \\
-4 & 0 & 0 & 0 & 4 & 0 & -1\tfrac{1}{3} & 0 & 0 & 2\tfrac{2}{3} & -1\tfrac{1}{3} & 0 \\
4 & 0 & 0 & 4 & 0 & 0 & -1\tfrac{1}{3} & 0 & 0 & -1\tfrac{1}{3} & 2\tfrac{2}{3} & 0 \\
0 & -4 & 0 & 0 & 0 & 4 & 0 & -1\tfrac{1}{3} & 0 & 0 & 2\tfrac{2}{3} & -1\tfrac{1}{3} \\
0 & 4 & 0 & 0 & 4 & 0 & 0 & -1\tfrac{1}{3} & 0 & 0 & -1\tfrac{1}{3} & 2\tfrac{2}{3} \\
0 & 0 & -4 & 0 & 0 & 4 & 0 & 0 & -1\tfrac{1}{3} & 2\tfrac{2}{3} & 0 & -1\tfrac{1}{3} \\
0 & 0 & 4 & 4 & 0 & 0 & 0 & 0 & -1\tfrac{1}{3} & -1\tfrac{1}{3} & 0 & 2\tfrac{2}{3}
\end{bmatrix}$$

For example, shape function $\theta_0 = \phi_0 + 4\phi_{12} - 4\phi_{13} + 4\phi_{14} - 4\phi_{15}$ owns the δ-property $L_i(\theta_0) = \delta_{i,0}$ and DOF $c_{12}(p) = 4L_0(p) - 4L_1(p) + 1^1/_3 L_6(p) + 1^1/_3 L_7(p) - 2^2/_3 L_8(p) + L_{12}(p)$ corresponds to shape function ϕ_{12}.

Another way of constructing a new basis is to integrate the DOFs using exact integration, a reference basis for the polynomial space and then use the δ-property to obtain the linear combination of the reference basis (see P. Monk, page 140).

The δ-property is used to eliminate the DOFs corresponding to the essential boundary conditions from the system.

3.4 PML

The PML takes care of damping incoming (reflected) waves. The coordinates perpendicular to the boundary is stretched by a complex number

$$\tilde{x} = x + i \int_0^x \sigma(\xi)\, d\xi,\ d\tilde{x} = (1 + i\sigma)dx = \gamma dx,$$

where the real functions σ is defined as

$$\sigma(\xi) = \begin{cases} \sigma^* \left(\frac{\xi - x_0}{x_1 - x_0}\right)^2 & x_0 < \xi < x_1 \\ 0 & \xi < x_0 \end{cases},$$

for some real constant σ^*, an upper bound x_0 and a lower bound x_1. Generally, we have mapping G

$$G : x \to \tilde{x}.$$

3.4.1 Maxwell equations

The electric field transforms as

$$\tilde{E} \circ G = \mathrm{d}G^{-T} E.$$

The idea is that E is continued into the upper half of the complex plane in each direction, so that

$$\tilde{\nabla} \times (\tilde{\nabla} \times \tilde{E}) - 4\pi^2 n_i^2 \tilde{E} = \tilde{F}.$$

If we change back to the physical coordinates we derive that

$$(\tilde{\nabla} \times \tilde{u}) \circ G = A \nabla \times B\tilde{u},$$

with $A = (\det(\mathrm{d}G))^{-1} \mathrm{d}G$ and $B = \mathrm{d}G^T$ given by

$$A = \begin{bmatrix} \frac{1}{\gamma_2\gamma_3} & 0 & 0 \\ 0 & \frac{1}{\gamma_1\gamma_3} & 0 \\ 0 & 0 & \frac{1}{\gamma_1\gamma_2} \end{bmatrix}, \; B = \begin{bmatrix} \gamma_1 & 0 & 0 \\ 0 & \gamma_2 & 0 \\ 0 & 0 & \gamma_3 \end{bmatrix}.$$

From the new variable $\bar{E} = B\tilde{E}$ and right-hand side $\bar{F} = B\tilde{F}$ we obtain

$$\nabla \times (\mu^{-1}\nabla \times \bar{E}) - 4\pi^2 n_i^2 \mu \bar{E} = \mu \bar{F},$$

with

$$\mu = (BA)^{-1} = \begin{bmatrix} \frac{\gamma_2\gamma_3}{\gamma_1} & 0 & 0 \\ 0 & \frac{\gamma_1\gamma_3}{\gamma_2} & 0 \\ 0 & 0 & \frac{\gamma_1\gamma_2}{\gamma_3} \end{bmatrix}.$$

Note that $\bar{E}$ matches E at the interface of the PML because $\gamma_3(z) = 1$ at the interface.

3.4.2 Variational formulation

The variational formulation in the PML region will be (Monk, page 378)

$$\int_\Omega (\mu^{-1}\nabla \times \bar{E}) \cdot (\nabla \times \phi) - 4\pi^2 n_i^2 \mu \bar{E}\phi dV + \oint \sigma \bar{E}_T \phi_T d\Gamma = \oint \bar{r}\phi_T d\Gamma + \int_\Omega \mu \bar{F}\phi dV.$$

3.4.3 Boundary conditions

The corresponding boundary condition in the PML is (Monk, page 381)

$$n \times (\mu^{-1}\nabla \times \bar{E}) = \sigma \bar{E}_T - \bar{r},$$

where $\bar{r}$ should be derived from the known (stretched) incident wave

$$\bar{r} = -n \times (\mu^{-1}\nabla \times \bar{E}^{\text{inc}}) + \sigma \bar{E}_T^{\text{inc}}.$$

3.5 Constraints

Direchlet and periodic boundary conditions can be looked upon as constraints to the DOFs. Suppose the mass matrix is constructed straightforward following the variational formulation, resulting in the linear system

$$Ax = b,$$

where x are the DOFs corresponding to the functional space $\{\phi_i\}$. The constraint equation for the boundary conditions is an affine function

$$x = Cy + d,$$

where C is a non-square complex-valued matrix and d a vector. DOFs y correspond to functional subspace $\{\Phi_j\} \subseteq \{\phi_i\}$ (where the boundary DOFs are eliminated).

3.5.1 Boundary conditions

Recall the expansion formula

$$E = \sum_{i=1}^{N} \phi_i x_i, \quad x_i = L_i(E),$$

and in terms of the functions in subspace ($M \leq N$) you also may write

$$E = \sum_{j=1}^{M} \Phi_j y_j$$

and the DOFs are related by

$$x_i = L_i(E) = L_i\left(\sum_{j=1}^{M} \Phi_j y_j\right) = \sum_{j=1}^{M} L_i(\Phi_j) y_j = \sum_{j=1}^{M} C_{ij} y_j.$$

Dirichlet boundary condition at location N (spanned by ϕ_N) in constraint form is $x_N = L_N(E) = d$ and $L_N(\Phi_j) = 0$, which gives $C_{Nj} = 0$, $d_N = d$. A similar constraint can be found for the periodic boundary conditions. For example, construct the function $\Phi_1 = \phi_1 + \phi_N$, a linear combination of the original base functions at the boundaries, and apply the expansion above. This gives $C_{11} = L_1(\Phi_1) = L_1(\phi_1) = 1$ and $C_{N1} = L_N(\phi_N) = 1$.

3.5.2 Reduced system

The above system is solved by eliminating the constraint function for x and solving the following system for y

$$C^H ACy = C^H b - C^H Ad.$$

3.6 Errors

The error defined in the $H(\text{curl};\Omega)$ space is defined as

$$\begin{aligned} \left\|E - E^{\text{exact}}\right\|_{H(\text{curl};\Omega)} = \\ \left\|E - E^{\text{exact}}\right\|^2_{(L^2(\Omega))^3} + \left\|\nabla \times (E - E^{\text{exact}})\right\|^2_{(L^2(\Omega))^3} = \\ (x - x^{\text{exact}})^H A(x - x^{\text{exact}}), \end{aligned}$$

where x is the vector of DOFs and A is a mass matrix of the system with natural boundary conditions $n \times (\nabla \times E) = 0$.

The relative error is defined as

$$\frac{\|E - E^{\text{exact}}\|_{H(\text{curl};\Omega)}}{\|E^{\text{exact}}\|_{H(\text{curl};\Omega)}}.$$

Error estimates can be obtained by restriction on the coefficients in the problem (Monk, pages 169 and 277).

3.7 Preconditioners

Preconditioners are used to design faster iterative solvers such as algebraic MG methods. The motivation to use Nested Multigrid Potential Preconditioner (NMGAV) preconditioner is the slow convergence of the FEM system. The first reason is the presence of non-zero gradient components or spurious modes and the resolution of the low-frequency modes (Zhu & Cangellaris, page 160). Two types of linear subspaces are used in this algorithm and need transfer operators to project them to the original space and vice versa.

Basically, define a linear subspace V of the solution space W and construct a transfer operator G

$$V = WG,$$

where W and V is a row vector of the base functions that spans the consecutive spaces.

If an approximated solution x_W for system $A(W^T, W)x_W = f_W$ is obtained, we solve the following preconditioned system

$$A(V^T, V)x_v = G^T(f_W - A(W^T, W)x_W).$$

and correct x_W as

$$x_w \mapsto x_w + Gx_v.$$

For the Maxwell equations the two types of subspaces are gradient space $\nabla W^i \subset W^i$ and the coarse grid spaces $W^i_{kh} \subset W^i_{(k-1)h} \subset \cdots \subset W^i_h$.

3.7.1 Potential formulation

In the case of the gradient subspace ∇W, we formulate the potential formulation of the problem. It follows from the Gauss' electric field law constraining the solution (Zhu & Cangellaris, page 167) (non-dimensional)

$$\nabla \cdot (\epsilon_r E) = \frac{1}{2\pi i} \nabla \cdot J_v,$$

with J_v is the electric current density with boundary condition $J_v \cdot n = 0$.

We construct the weak formulation by multiplying it with the test function $\phi \in \nabla W$:

$$\int_\Omega \nabla \cdot (\epsilon_r E)\phi \, dV = \frac{1}{2\pi i} \int_\Omega \nabla \cdot J_v \phi \, dV$$

and $E \in \nabla W$. Partial integration gives

$$\int_\Omega \nabla \cdot (\epsilon_r E\phi) - \epsilon_r E \cdot \nabla\phi \, dV = \frac{1}{2\pi i} \int_\Omega \nabla \cdot (J_v\phi) - J_v \cdot \nabla\phi \, dV.$$

On the first part on both sides we can apply divergence theorem

$$\int_\Omega \nabla \cdot (\epsilon_r E\phi) = \oint_{\partial\Omega} \epsilon_r E \cdot n\phi \, dS$$

and the zero term (boundary condition for J_v)

$$\int_\Omega \nabla \cdot (J_v \phi) = \oint_{\partial\Omega} J_v \cdot n\phi \, dS = 0.$$

Using the Ampère and Faraday relations, again the boundary conditions $J_v \cdot n = 0$, $\phi = 0$ and a vector identity, the right-hand side integral can be rewritten as (Zhu & Cangellaris, page 167, non-dimensional)

$$\oint_{\partial\Omega} \epsilon_r E \cdot n\phi \, dS = \frac{1}{2\pi i} \oint_{\partial\Omega} (J_v - \nabla \times H) \cdot n\phi \, dS =$$

$$\frac{-1}{2\pi i} \oint_{\partial\Omega} n \times H \cdot \nabla\phi \, dS = \frac{-1}{2\pi i \mu_r} \oint_{\partial\Omega} n \times \nabla \times E \cdot \nabla\phi \, dS$$

This multiplied by $2\pi i \mu_r$, we get the divergence free constraint

$$-4\pi^2 n_i^2 \int_\Omega E \cdot \nabla\phi \, dV + \oint_{\partial\Omega} n \times \nabla \times E \cdot \nabla\phi \, dS = 2\pi i \mu_r \int_\Omega J_v \cdot \nabla\phi \, dV.$$

Including the Robin boundary condition we finally have

$$-4\pi^2 n_i^2 \int_\Omega E \cdot \nabla\phi \, dV + \oint_{\partial\Omega} \sigma E_T \cdot \nabla\phi \, dS - \oint_{\partial\Omega} r \cdot \nabla\phi \, dS = 2\pi i \mu_r \int_\Omega J_v \cdot \nabla\phi \, dV.$$

The PML can easily be included

$$-4\pi^2 n_i^2 \int_\Omega \mu \bar{E} \cdot \nabla\phi \, dV + \oint_{\partial\Omega} \sigma \bar{E}_T \cdot \nabla\phi \, dS - \oint_{\partial\Omega} \bar{r} \cdot \nabla\phi \, dS = \int \mu \bar{F} \cdot \nabla\phi \, dV.$$

From this, the potential formulation is in fact the same equation as the field formulation (Zhu & Cangellaris, page 181), i.e.

$$A(\nabla W^T, \nabla W) = G^T A(W^T, W) G$$

$$f_{\nabla W}(\nabla W^T) = G^T f_W$$

$$x_W = G x_{\nabla W}.$$

3.7.2 Multigrid

The finite element is divided into subelements and the corresponding base functions form a linear subspace.

The algorithm (Zhu & Cangellaris, page 170) for NMGAV

$$x_W^h \leftarrow NMGAV(f_E^h, n = 1),$$

where the superscript h denotes the finest grid $n = 1$ and the coarsest grid is Nh.

1. if $n = N$, solve the curl formulation exactly.
2. else
   (a) pre-smooth v times on the potential formulation
      i. pre-smooth curl formulation using forward GS v times
      ii. calculate new right-hand side $f_{\nabla W} \leftarrow G^T(f_W^{nh} - Ax_W^{nh})$
      iii. pre-smooth on potential formulation using forward GS v times
      iv. correct electric field $x_W^{nh} \leftarrow x_W^{nh} + G\, x_{\nabla W}$
   (b) calculate new right-hand side $f_W^{(n+1)h} \leftarrow Q^T(f_W^{nh} - Ax_W^{nh})$
   (c) $x_W^{(n+1)h} \leftarrow NMGVA(f_W^{(n+1)h}, n + 1)$
   (d) $x_W^{nh} \leftarrow x_W^{nh} + Q\, x_W^{(n+1)h}$
   (e) Post-smooth v times on the potential formulation
      i. calculate new right-hand side $f_{\nabla W} \leftarrow G^T(f_W^{nh} - Ax_W^{nh})$, $x_{\nabla W} \leftarrow 0$
      ii. post-smooth on potential formulation using backward GS v times
      iii. calculate new right-hand side $f_W^{nh} = f_W^{nh} - AG\, x_{\nabla W}$
      iv. post-smooth on curl formulation using backward GS v times
      v. correct electric field $x_W^{nh} \leftarrow x_W^{nh} + G\, x_{\nabla W}$

Discarding steps 2(a)iv, 2(b), 2(c), 2(d) and 2(e)i in the above algorithm renders the single grid potential preconditioner (SGAV, Zhu & Cangellaris page 168).

4 Implementation

The previous section give the general algorithm. The following subsections cover in more detail the choices made in the implementation stage.

4.1 Boundary conditions

4.1.1 Silver-Müller

For the general incident wave, we assume that zero modes are dominant and approximate the scattered field at the top boundary to

$$E^{\text{scat}} \approx q \exp(-2\pi i n_0 d \cdot x).$$

Which means we have to look for a suitable σ such that $n \times (\nabla \times E^{\text{scat}}) = \sigma n \times (E^{\text{scat}} \times n)$. The curl of E^{scat}, $\nabla \times E^{\text{scat}} = -2\pi i n_0 d \times E^{\text{scat}}$, and assume almost perpendicular incident waves $d \approx -n$, we approximate $\sigma = -2\pi i n_0$.

For example for TE polarization in 2D, the plane wave incident field

$$E_2^{\text{inc}}(x, y, z) = B_0 \exp(-2\pi i n_0 z),$$

$$E_1^{\text{inc}} = E_3^{\text{inc}} = 0$$

is a solution of the Maxwell equation. At $z = M$, the electric field E satisfies

$$\frac{\partial E_2}{\partial z} - 2\pi i n_0 E_2 = -2\pi i 2 n_0 B_0 \exp(-2\pi i n_0 z),$$

$$E_1 = E_3 = 0.$$

At $z = 0$, we have

$$-\frac{\partial E_2}{\partial z} - 2\pi i n_3 E_2 = 0,$$

$$E_1 = E_3 = 0.$$

For the scattered field formulation with E^{inc} subtracted on the whole domain we get at the top

$$\frac{\partial E_2^{\text{scat}}}{\partial z} - 2\pi i n_0 E_2^{\text{scat}} = 0,$$

$$E_1 = E_3 = 0$$

and at the bottom

$$-\frac{\partial E_2^{\text{scat}}}{\partial z} - 2\pi i n_0 E_2^{\text{scat}} = -2\pi i (n_0 - n_3) E^{\text{inc}},$$

$$E_1 = E_3 = 0.$$

4.1.2 PEC

A PEC boundary can be implemented as a homogeneous Dirichlet boundary condition for the DOFs (in the function space these are the tangential parts of the field E).

4.2 PML

The PML is basically a material with anisotropic properties, which must be chosen carefully. As the problem is described by the Maxwell equations it requires a boundary conditions.

4.2.1 Parameters

The scattered field inside the PML is multiplied by a function

$$\exp\left(-2\pi n_0 \int_{z_0}^{z} \sigma_3(\xi) d\xi\right).$$

The rule of thumb is that $\int_{z_0}^{z} \sigma_3(\xi)\, d\xi$ should be constant for varying PML layer thickness. The constant σ^* cannot be taken too large, because the incident wave amplitude increases exponentially towards the boundary of the domain, which requires a finer mesh.

4.2.2 Boundary conditions

A PML is supposed to damp out all waves in a certain direction and if the it performs well, PEC conditions would suffice. But the radiation condition is also a good choice. We construct the equation which describes the scattered wave $\tilde{E}^{\text{scat}}$ approximately at the boundary as

$$n \times (\tilde{\nabla} \times \tilde{E}^{\text{scat}}) + 2\pi i n_0 \tilde{E}_T^{\text{scat}} = 0.$$

The boundary condition becomes at the top $n = [0, 0, 1]^T$:

$$\begin{bmatrix} \frac{\partial \tilde{E}_3}{\partial \tilde{x}} - \frac{\partial \tilde{E}_1}{\partial \tilde{z}} \\ \frac{\partial \tilde{E}_3}{\partial \tilde{y}} - \frac{\partial \tilde{E}_2}{\partial \tilde{z}} \\ 0 \end{bmatrix} = -2\pi i n_0 \begin{bmatrix} -\tilde{E}_1 \\ \tilde{E}_2 \\ 0 \end{bmatrix} - \tilde{r}$$

For the planar wave with $\theta = 0$, $\phi = 0$ and $\psi = \pi/2$, at $\tilde{z} = \tilde{M}$, we have:

$$\tilde{E}_1 = \tilde{E}_3 = 0,$$

$$\frac{\partial \tilde{E}_2}{\partial \tilde{z}} - 2\pi i n_0 \tilde{E}_2 = -2\pi i 2 n_0 B_0 \exp(-2\pi i n_0 \tilde{z}),$$

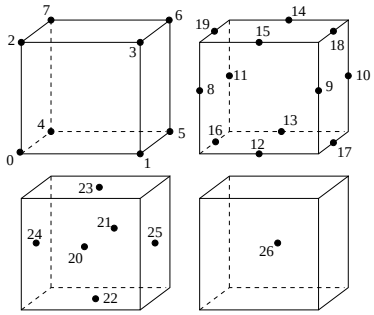

Figure 6: (Re)numbering nodes for a 3x3x3 mesh with 3 periodic boundary conditions.

which means $\sigma = -2\pi i n_0$ and $\tilde{r} = -2\pi i 2 n_0 B_0 \exp(-2\pi i n_0 \tilde{z})$ in this case.

And at $\tilde{z} = 0$, we simply have

$$\tilde{E}_1 = \tilde{E}_3 = 0$$

$$-\frac{\partial \tilde{E}_2}{\partial \tilde{z}} - 2\pi i n_3 \tilde{E}_2 = 0,$$

so $\sigma = -2\pi i n_3$ and $\tilde{r} = 0$.

4.3 Orientation

Important is the direction of the tangential vectors defining edges. The directions should be the same for each (tetrahedral) element sharing the same face. The local vertex renumbering in these corresponding elements define the directions uniquely. Also the numbering of vertices on the matching faces at the corresponding periodic boundaries should count for the correct orientation of the edge and face DOFs. This is achieved by first renumbering the corners (at least six periodic boundaries), edges (at least 4 periodic boundaries) and faces (at least 2 periodic boundaries) as depicted in Figure 6.

4.4 Constraints

Grating retain the full solution vector $x^T = [y\ z]^T$, where $y = Qx$ are the unconstraint DOFs and $z = Px$ are the constraint DOFs. The system including the constraint equation is solved

$$\begin{bmatrix} C^H A C & 0 \\ -PC & I \end{bmatrix} \begin{bmatrix} y \\ z \end{bmatrix} = \begin{bmatrix} C^H b - C^H A d \\ Pd \end{bmatrix}.$$

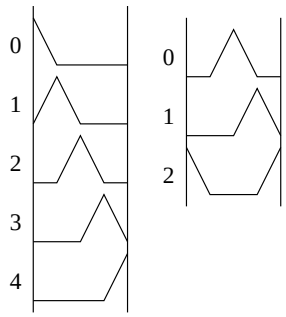

Figure 7: Linear subspace

Let's eliminate the quasi-periodic boundary condition $x_0 = \alpha x_1$ where x_1 is a unconstrained DOF. If the base function Φ_0 is defined as the linear combination of two original base functions $\Phi_0 = \alpha\phi_0 + \phi_1$, and copying the other base functions $\Phi_j = \phi_{j+1}, j \geq 1$ we can write $E = y_0\Phi_0 + y_1\Phi_1 + \cdots = y_0\alpha\phi_0 + y_0\phi_1 + y_1\phi_2 \cdots$. Then the DOFs y and z are directly related to the DOFs x as

$$\begin{aligned} y_0 &= x_1 \\ y_1 &= x_2 \\ &\cdots \\ z_0 = x_0 &= y_0\alpha, \end{aligned}$$

The (non-square) matrix Q has a the identity at the unconstrained rows and zeros elsewhere. For more general boundary conditions, the constraints are written as

$$x_i = \sum_{j \neq i} \alpha_{ij} x_j + \beta_i,$$

where α_{ij}, β_i are complex numbers, there is also a direct correspondence (i.e. $C_{ij} = \alpha_{ij}$ and $d_i = \beta_i$).

An illustrative example with one Dirichlet and one periodic boundary condition

A standard nodal finite element space W contains 5 base functions, numbered from 0 to 4. The new space $V \subset W$ is a linear subspace, in which the base functions are linear combinations of the original ones. Note that base function 1 in W is located on a Dirichlet boundary and is therefore eliminated. The transfer matrix C in $V = WC$ is

$$C = \begin{bmatrix} 0 & 0 & 1 \\ 0 & 0 & 0 \\ 1 & 0 & 0 \\ 0 & 1 & 0 \\ 0 & 0 & 1 \end{bmatrix}$$

and P and Q are defined as

$$P = \begin{bmatrix} 1 & 0 & 0 & 0 & 0 \\ 0 & 1 & 0 & 0 & 0 \end{bmatrix}, Q = \begin{bmatrix} 0 & 0 & 1 & 0 & 0 \\ 0 & 0 & 0 & 1 & 0 \\ 0 & 0 & 0 & 0 & 1 \end{bmatrix}.$$

In case of vector base functions, the periodic boundary conditions also involve the difficulty of orientation. The pair of DOFs, say x_0 and x_1, need to be identified and corrected for orientation. Since the mesh is unstructured, we have to consider the orientation of both element and edge. By smart numbering all the orientations are equal at both sides: first number the eight corner vertices, the vertices on the 10 edges and the other vertices on the 6 sides of the domain, respectively.

4.5 Finite elements

Below a number of vector elements from the first family are discussed.

4.5.1 Whitney

A DOF is defined on an edge, which are shared by the neighboring elements. On a element, the middle nodes are shared this way. So, the vertices have no DOFs and middle points ($i = 0, ..., 5$) are the location of the edge element DOFs.

4.5.2 Second order Nedelec

20 shape functions define the solution. So, in addition to the Whitney functions, 6 extra edge functions ($i = 0, ..., 11$) and 8 face functions ($i = 12, ..., 19$) are implemented. Note that $i = 0$ and $i = 1$ are a Whitney and a linear edge functions defined on edge e_0, and so on. Face nodes are located in the centre of the faces. The delta property for this element is forced by the explicitly do the linear combination as described above.

4.5.3 Third order Nedelec

45 shape functions are implemented. Adding 6 edge functions ($i = 0, ..., 17$), 16 face functions ($i = 18, ..., 41$) and 3 volume functions ($i = 42, ..., 44$) to the second order Nedelec shape functions. The volume DOFs are part of the element itself, so no node (or location) is associated to these DOFs.

4.6 Constraints

The constrained DOFs are eliminated from the mass matrix and right-hand side, but kept in the system as linear combination of other DOFs. What is the impact of applying transfer operators on these systems.

Suppose we have two constraint equations $x = Cy+d$, $\hat{x} = \hat{C}\hat{y}+\hat{d}$ and a transfer operator G that maps to these equations

$$x = G\hat{x}.$$

Thus,

$$Cy + d = G(\hat{C}\hat{y} + \hat{d}).$$

The constrained preconditioned system can be derived

$$A(Cy + d) = b$$

$$AG(\hat{C}\hat{y} + \hat{d}) = b$$

$$AG\hat{C}\hat{y} = b - AG\hat{d}$$

$$(G\hat{C})^T AG\hat{C}\hat{y} = (G\hat{C})^T(b - AG\hat{d})$$

$$\hat{C}^T(G^T AG)\hat{C}\hat{y} = \hat{C}^T G^T b - \hat{C}^T(G^T AG)\hat{d}$$

$$\hat{C}^T \hat{A}\hat{C}\hat{y} = \hat{C}^T \hat{b} - \hat{C}^T \hat{A}\hat{d}$$

Which means that constraining is effectively a multiplicative combination of two preconditioners $\hat{C}$,G and the constraint part of the system remains decoupled.

Can we construct a transfer operator for the constrained variables y and $\hat{y}$? Note that $d = G\hat{d}$ holds, so

$$Cy = G\hat{C}\hat{y}.$$

If multiplied with the transpose of C, the right-hand side operator is the constrained transfer operator

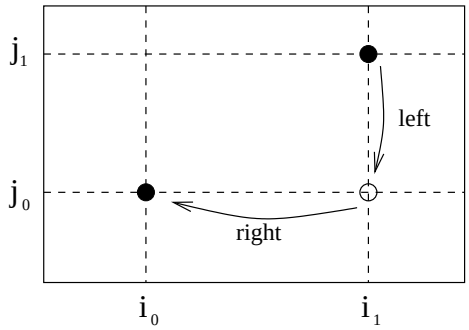

Figure 8: Reposition of elements by constraining. Left and right multiplication.

Figure 9: Periodic base functions.

$$C^H C y = C^H G \hat{C} \hat{y}.$$

In the case of Dirichlet boundary conditions $C^H C = I$, the identity matrix. For quasi-periodic boundaries this product is a diagonal matrix and in the general case a full matrix. Note that in all cases $C^H C$ is invertible. So the operator $\hat{G}$ transferring y to $\hat{y}$ is

$$\hat{G} = \left(C^H C\right)^{-1} C^H G \hat{C}.$$

In the assembly stage the problem of a non-unit diagonal element is circumvented by *overwriting* the entries in the operator, this is automatically achieved by the in-lined constraining as done in Grating.

Left and right multiplying the transfer matrix with the constraints will reposition the contributions. The quasi-periodic boundary conditions as defined above will ensure that the factor is always 1 (i.e. the complex constraint is only a shift in the angle).

4.7 Preconditioner

As an example, the NMGAV algorithm uses the spaces $\nabla W = \{\nabla\lambda_0, \nabla\lambda_1, \nabla\lambda_2, \nabla\lambda_3\}$, where λ_i are the barycentric coordinates and $W = \{\phi_0, \phi_1, \phi_2, \phi_3, \phi_4, \phi_5\}$ the approximation space of lowest order Whitney elements (e.g. $\phi_0 = \lambda_0\nabla\lambda_1 - \lambda_1\nabla\lambda_0$, ...), then $G_{ij} = L_i(\nabla\lambda_j)$:

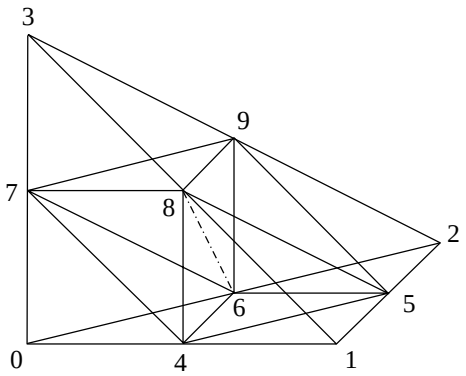

Figure 10: Division tetrahedron

$$G = \begin{bmatrix} -1 & 1 & 0 & 0 \\ 0 & -1 & 1 & 0 \\ -1 & 0 & 1 & 0 \\ -1 & 0 & 0 & 1 \\ 0 & -1 & 0 & 1 \\ 0 & 0 & -1 & 1 \end{bmatrix}.$$

The elements on the coarse grid are divided into 8 sub-elements

with numbering 0-4-6-7, 4-1-5-8, 6-5-2-9, 7-8-9-3, 4-5-6-8, 7-4-6-8, 6-8-5-9 and 7-8-6-9, respectively.

The numbering of the sub-elements is such that the sorted numbering on the outer sides of the sub-elements is preserved. So, for sub-element 0-4-6-7, sides s_0, s_1 and s_3 has the local 0-1-2, 0-1-3 and 0-2-3 numbering respectively. This is needed for identifying the new boundary faces.

5 Results

The results listed below are obtained from simple configurations with analytical solutions.

5.1 Two-layer problem

The two-layer problem with is a prescribed incident plane wave that reflects back a part of this wave. The exact solution (Pomplun, page 10) is used to determine the convergence behavior.

The solution can be written as a number of plane waves $E_0 = E_{A_0} + E_{B_0}$ and $E_1 = E_{A_1}$ with

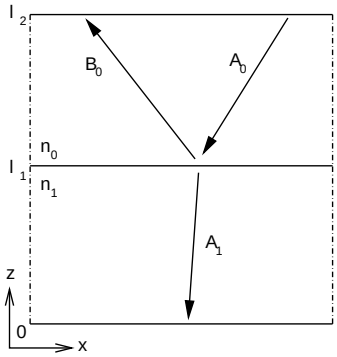

Figure 11: Exact solution two-layer case

$$E_{A_0}(x) = A_0 \exp(2\pi i n_0 d_{A_0} \cdot x),$$

$$E_{B_0}(x) = B_0 \exp(2\pi i n_0 d_{B_0} \cdot x),$$

$$E_{A_1}(x) = A_1 \exp(2\pi i n_1 d_{A_1} \cdot x),$$

where

$$A_0 \cdot d_{A_0} = B_0 \cdot d_{B_0} = A_1 \cdot d_{A_1} = 0$$

The outgoing wave is reflected back at the same angle

$$(d_{B_0})_x = (d_{A_0})_x,\ (d_{B_0})_y = (d_{A_0})_y,\ (d_{B_0})_z = -(d_{A_0})_z,$$

and from the refraction preservation we have

$$n_1(d_{A_1})_x = n_0(d_{A_0})_x,\ n_1(d_{A_1})_y = n_0(d_{A_0})_y,$$

$$(d_{A_1})_z = -\sqrt{1 - (d_{A_1})_x^2 - (d_{A_1})_y^2}.$$

We take the minus sign here, because we are interested in (the physical) waves going toward $z \to -\infty$.

At the interface $z = l_1$ we have $n \times (E_0 - E_1) = 0$, thus

$$(A_0)_{x,y} \exp(2\pi i n_0 (d_{A_0})_z l_1) + (B_0)_{x,y} \exp(2\pi i n_0 (d_{B_0})_z l_1) = (A_1)_{x,y} \exp(2\pi i n_1 (d_{A_1})_z l_1).$$

And $n \times (\nabla \times E_0 - \nabla \times E_1) = 0$. Using the identity $\nabla \times E = 2\pi i n_i d \times E$, we have

$$n_0(d_{A_0} \times A_0)_{x,y} \exp(2\pi i n_0 (d_{A_0})_z l_1) + n_0(d_{B_0} \times B_0)_{x,y} \exp(2\pi i n_0 (d_{B_0})_z l_1)$$

$$= n_1(d_{A_1} \times A_1)_{x,y} \exp(2\pi i n_1 (d_{A_1})_z l_1).$$

For the six unknowns A_1 and B_0 we have six linear equations, which can be solved:

$$\begin{bmatrix} (d_{A_1})_x & (d_{A_1})_y & (d_{A_1})_z & 0 & 0 & 0 \\ 0 & 0 & 0 & (d_{B_0})_x & (d_{B_0})_y & (d_{B_0})_z \\ \alpha & 0 & 0 & -\beta & 0 & 0 \\ 0 & \alpha & 0 & 0 & -\beta & 0 \\ 0 & -n_1(d_{A_1})_z\alpha & n_1(d_{A_1})_y\alpha & 0 & n_0(d_{B_0})_z\beta & -n_0(d_{B_0})_y\beta \\ n_1(d_{A_1})_z\alpha & 0 & -n_1(d_{A_1})_x\alpha & -n_0(d_{B_0})_z\beta & 0 & n_0(d_{B_0})_x\beta \end{bmatrix} \begin{bmatrix} (A_1)_x \\ (A_1)_y \\ (A_1)_z \\ (B_0)_x \\ (B_0)_y \\ (B_0)_z \end{bmatrix} =$$

$$[0, 0, \gamma(A_0)_x, \gamma(A_0)_y, \gamma n_0(d_{A_0} \times A_0)_x, \gamma n_0(d_{A_0} \times A_0)_y]^T$$

with $\alpha = \exp(2\pi i n_1 (d_{A_1})_z l_1)$, $\beta = \exp(2\pi i n_0 (d_{B_0})_z l_1)$ and $\gamma = \exp(2\pi i n_0 (d_{A_0})_z l_1)$. This linear system can be solved numerically (LU-decomposition) for a given incident wave. For example $n_0 = 1$, $n_1 = 2$, $l_1 = \frac{1}{2}$ with perpendicular incident wave $d_{A_0} = [0, 0, -1]^T$ and $A_0 = [0, 1, 0]^T$, we get $B_0 = [0, -\frac{1}{3}, 0]^T$, $A_1 = [0, -\frac{2}{3}, 0]^T$, $d_{B_0} = [0, 0, 1]^T$ and $d_{A_1} = [0, 0, -1]^T$.

Note that the solution for this problem can be obtained without solving the linear system above. We can reduce the problem a one-dimensional problem for TE and TM type waves. If we rotate the coordinate system around the z-axis, the y-components of the electric and magnetic field decouples, $E_y = e_y(z) \exp(\pm i k_{x'} x')$ and $H_y = h_y(z) \exp(\pm i k_{x'} x')$. In our problem the rotation is $x = x' \cos(\phi)$ and $y = x' \sin(\phi)$. Furthermore, we have $e_y^{\text{inc}}(z) = p_y \exp(-2\pi i n_0 \cos(\theta) z)$ for the incoming wave.

Then use the Fresnel reflection and transmission coefficients (part 2; Chew, page 48) and impose constraints on the interfaces to obtain the amplitudes of the $e_y(z)$ in the different layers.

For TE waves the traverse components E_z and E_x are then calculated from $p \cdot d = 0$ and $p_z = 0$.

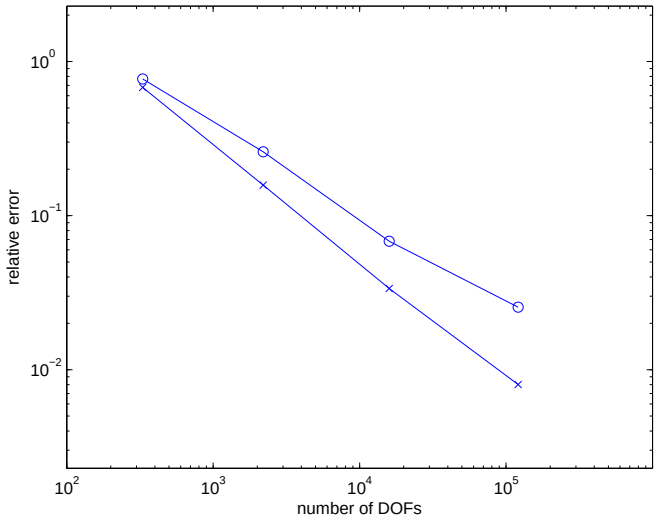

Figure 12: $\circ$ error $H(\text{curl})$-norm and $\times$ L_2-norm two-layer problem. Uniform mesh, Whitney elements.

5.2 Cavity problem

Figure 13 shows the result the simulation of the cavity problem. It has the solution

$$E^{\text{exact}} = p \exp(2\pi i d \cdot x),$$

where $p \cdot d = 0$ and d is a unit vector. It satisfies the Maxwell equations with $F = 0$ and $n_i = 1$.

The solution to the second problem is an element in $R_1 = \left\{u(x) = a + b \times x \mid a, b \in \mathbb{C}^2\right\}$:

$$E^{\text{exact}} = \begin{bmatrix} y - z \\ 4 - (x - z) \\ x - y \end{bmatrix},$$

with $\nabla \times \nabla \times E^{\text{exact}} = 0$ and should be resolved exactly, when using Whitney elements (Monk, page 139).

$$E^{\text{exact}} = \begin{bmatrix} z^2 - xy \\ x^2 - zy \\ y^2 - xz \end{bmatrix}$$

is a function in $R_2 = (P_1)^3 \oplus S_2$ in which elements of S_2 are polynomials like xy, z^2. This function resolved exactly by second order elements. In this case,

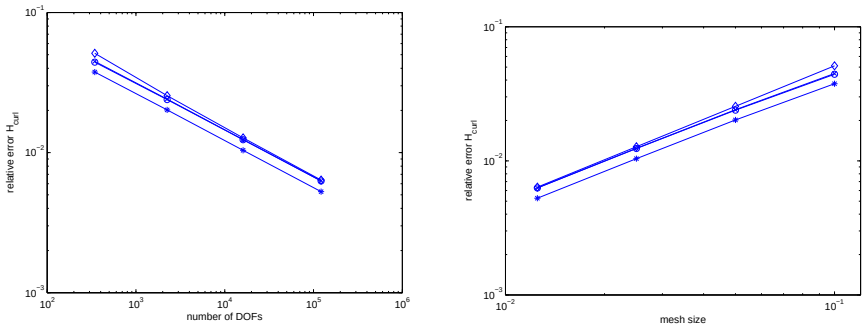

Figure 13: Error $H(\mathrm{curl})$-norm cavity problem. $\circ$ Dirichlet; $\times$ x-periodic; $\diamond$ x, y-periodic; $*$ Dirichlet, $\theta = 20°$. Domain $K = 0.8$, $L = 0.2$ and $M = 0.2$. Uniform grid, Whitney elements.

$\nabla \times \nabla \times E^{\text{exact}} = [-3, -3, -3]^T$.where a perfectly conducting region is placed in air.

5.3 Cylinder problem

The exact scattered solution E^s for the infinite cylinder problem is (Balanis, page 603)

$$E_z^s(r, \phi) = -E_0 \sum_{n=0}^{\infty} \epsilon_n i^n \frac{J_n(ka)}{H_n^{(1)}(ka)} H_n^{(1)}(kr) \cos(n\phi),$$

where $\epsilon_0 = 1$, $\epsilon_n = 2$, $n > 0$. Hankel function of the first kind $H_n^{(1)}$ and J_n Bessel function of the first kind. k is the wave number and a is the radius of the cylinder.

5.4 Performance

Using the MKL PARDISO solver, we obtain a boost of factor 80 compared to the non-optimized PETSc direct LU solver. Note that PARDISO performs reordering for less fill-in (METIS), super node pivoting approach and maximum weighted matching algorithm. The convergence performance of the NMGAV algorithm is depicted in Figure 15 simulating the two-layer problem.

6 Appendix

Useful identities.

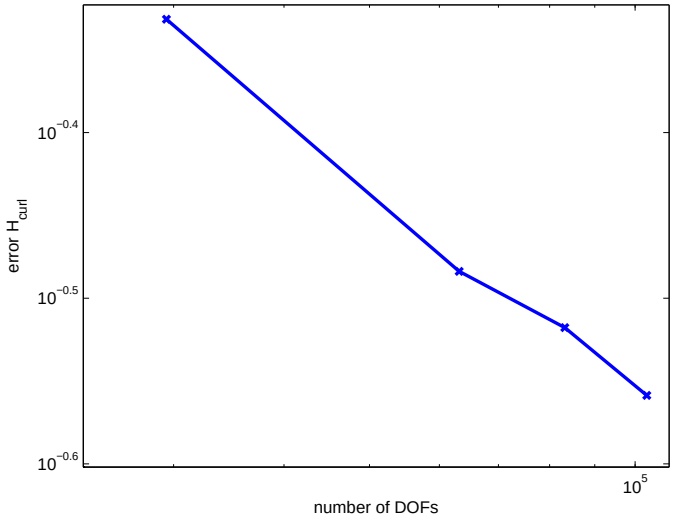

Figure 14: Error in $H(\mathrm{curl})$ of cylinder problem.

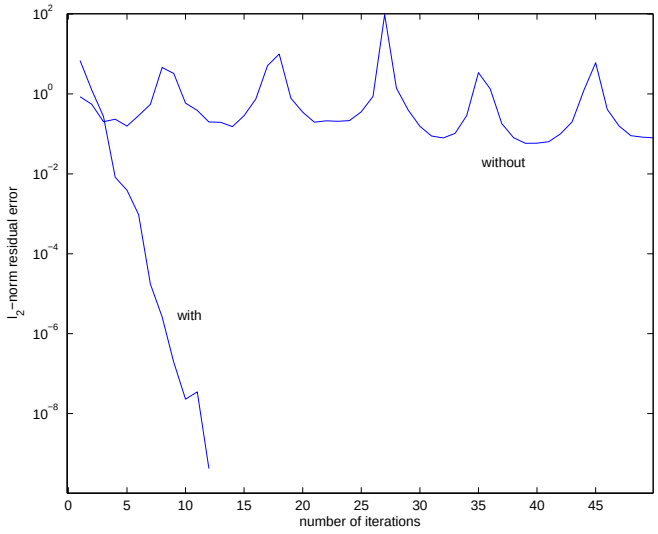

Figure 15: Convergence solver for two-layer problem with and without NMGAV-preconditioner.

6.1 Mapping

$$F(\hat{x},\hat{y},\hat{z}) = \begin{bmatrix} x(\hat{x},\hat{y},\hat{z}) \\ y(\hat{x},\hat{y},\hat{z}) \\ z(\hat{x},\hat{y},\hat{z}) \end{bmatrix}$$

$$\mathrm{d}F = \begin{bmatrix} \frac{\partial x}{\partial \hat{x}} & \frac{\partial x}{\partial \hat{y}} & \frac{\partial x}{\partial \hat{z}} \\ \frac{\partial y}{\partial \hat{x}} & \frac{\partial y}{\partial \hat{y}} & \frac{\partial y}{\partial \hat{z}} \\ \frac{\partial z}{\partial \hat{x}} & \frac{\partial z}{\partial \hat{y}} & \frac{\partial z}{\partial \hat{z}} \end{bmatrix}$$

$$(\mathrm{d}F)^{-T} = \begin{bmatrix} \frac{\partial \hat{x}}{\partial x} & \frac{\partial \hat{y}}{\partial x} & \frac{\partial \hat{z}}{\partial x} \\ \frac{\partial \hat{x}}{\partial y} & \frac{\partial \hat{y}}{\partial y} & \frac{\partial \hat{z}}{\partial y} \\ \frac{\partial \hat{x}}{\partial z} & \frac{\partial \hat{y}}{\partial z} & \frac{\partial \hat{z}}{\partial z} \end{bmatrix} = \frac{1}{\det(\mathrm{d}F)} \begin{bmatrix} \frac{\partial z}{\partial \hat{z}}\frac{\partial y}{\partial \hat{y}} - \frac{\partial z}{\partial \hat{y}}\frac{\partial y}{\partial \hat{z}} & -\left(\frac{\partial y}{\partial \hat{x}}\frac{\partial z}{\partial \hat{z}} - \frac{\partial y}{\partial \hat{z}}\frac{\partial z}{\partial \hat{x}}\right) & \frac{\partial y}{\partial \hat{x}}\frac{\partial z}{\partial \hat{y}} - \frac{\partial y}{\partial \hat{y}}\frac{\partial z}{\partial \hat{x}} \\ -\left(\frac{\partial x}{\partial \hat{y}}\frac{\partial z}{\partial \hat{z}} - \frac{\partial x}{\partial \hat{z}}\frac{\partial z}{\partial \hat{y}}\right) & \frac{\partial x}{\partial \hat{x}}\frac{\partial z}{\partial \hat{z}} - \frac{\partial x}{\partial \hat{z}}\frac{\partial z}{\partial \hat{x}} & -\left(\frac{\partial x}{\partial \hat{x}}\frac{\partial z}{\partial \hat{y}} - \frac{\partial x}{\partial \hat{y}}\frac{\partial z}{\partial \hat{x}}\right) \\ \frac{\partial x}{\partial \hat{y}}\frac{\partial y}{\partial \hat{z}} - \frac{\partial y}{\partial \hat{y}}\frac{\partial x}{\partial \hat{z}} & -\left(\frac{\partial x}{\partial \hat{x}}\frac{\partial y}{\partial \hat{z}} - \frac{\partial x}{\partial \hat{z}}\frac{\partial y}{\partial \hat{x}}\right) & \frac{\partial x}{\partial \hat{x}}\frac{\partial y}{\partial \hat{y}} - \frac{\partial y}{\partial \hat{x}}\frac{\partial x}{\partial \hat{y}} \end{bmatrix}$$

$$\det(\mathrm{d}F) = \frac{\partial x}{\partial \hat{x}}\left(\frac{\partial y}{\partial \hat{y}}\frac{\partial z}{\partial \hat{z}} - \frac{\partial z}{\partial \hat{y}}\frac{\partial y}{\partial \hat{z}}\right) + \frac{\partial y}{\partial \hat{x}}\left(\frac{\partial z}{\partial \hat{y}}\frac{\partial x}{\partial \hat{z}} - \frac{\partial x}{\partial \hat{y}}\frac{\partial z}{\partial \hat{z}}\right) + \frac{\partial z}{\partial \hat{x}}\left(\frac{\partial x}{\partial \hat{y}}\frac{\partial y}{\partial \hat{z}} - \frac{\partial y}{\partial \hat{y}}\frac{\partial x}{\partial \hat{z}}\right)$$

$$(\phi \circ F)(\hat{x}) = \phi(F(\hat{x}))$$

$$n \circ F = \frac{(\mathrm{d}F)^{-T}\hat{n}}{|(\mathrm{d}F)^{-T}\hat{n}|},\ \tau \circ F = \frac{\mathrm{d}F\,\hat{\tau}}{|\mathrm{d}F\,\hat{\tau}|}$$

$$\int_V \phi(x)\,\mathrm{d}V = \int_{\hat{V}} \phi(F(\hat{x}))|\det(\mathrm{d}F)|\,\mathrm{d}\hat{V}$$

$$\int_e \phi \mathrm{d}s = \int_a^b \phi(\mathbf{s}(t))\,\|\mathbf{s}'(t)\|\,\mathrm{d}t$$

$$S = r(T), \int_S \phi \mathrm{d}S = \int_T \phi[\mathbf{r}(u,v)]\left\|\frac{\partial \mathbf{r}}{\partial u} \times \frac{\partial \mathbf{r}}{\partial v}\right\| \mathrm{d}u\,\mathrm{d}v$$

6.2 Cross product and curl operator

$$a \times b = \begin{bmatrix} a_2 b_3 - a_3 b_2 \\ -(a_1 b_3 - a_3 b_1) \\ a_1 b_2 - a_2 b_1 \end{bmatrix}$$

$$a \cdot (b \times c) = (a \times b) \cdot c$$

$$(a + b) \times c = (a \times c) + (b \times c)$$

$$a \times b = -b \times a, \ (a \times b) \times a = a \times (b \times a)$$

$$a \times (b \times c) + b \times (c \times a) + c \times (a \times b) = 0$$

$$\nabla \times \nabla g = 0$$

$$\nabla \cdot (\nabla \times E) = 0$$

$$\nabla \cdot (A \times B) = B \cdot (\nabla \times A) - A \cdot (\nabla \times B)$$

$$A \times (B \times C) = (A \cdot C)B - (A \cdot B)C$$

$$\nabla \times (g\, F) = (\nabla g) \times F + g(\nabla \times F)$$

$$\nabla \cdot (g\, F) = g \nabla \cdot F + (\nabla g) \cdot F$$

$$A \cdot (\nabla \times \nabla \times B) - (\nabla \times \nabla \times A) \cdot B = \nabla \cdot (B \times \nabla \times A - A \times \nabla \times B)$$

$$\nabla \times E = \begin{bmatrix} \frac{\partial}{\partial y} E_3 - \frac{\partial}{\partial z} E_2 \\ -(\frac{\partial}{\partial x} E_3 - \frac{\partial}{\partial z} E_1) \\ \frac{\partial}{\partial x} E_2 - \frac{\partial}{\partial y} E_1 \end{bmatrix}$$

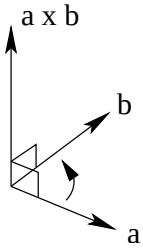

Figure 16: Cross product

References

[1] Peter Monk, “Finite Element Methods for Maxwell’s Equations”, Oxford University Press Inc., New York, ISBN 0 19 850888 3

[2] Yu Zhu and Andreas Cangellaris, “Multigrid Finite Element Methods for Electromagnetic Field Modelling”, The IEEE Press, Wiley-Interscience, ISBN 13 978 0 471 74110 7, ISBN 10 0 471 74110 8

[3] Weng Cho Chew, “Waves and Fields In Inhomogeneous Media”, Van Nostrand Reinhold, New York, ISBN 0 442 23816 9

[4] Constantine A. Balanis, “Advanced Engineering electromagnetics”, Wiley 1989, ISBN 0 471 62194 3

[5] Krzysztof A. Michalski, “Electromagnetic Scattering and radiation by surfaces of Arbitrary Shape in Layered Media, Part 1 & 2”, IEEE Trans. Antennas and Propagation, Vol. 38 Issue 3, 1990

[6] Pavel Solin, Karel Segeth, Ivo Dolezel, “Higher-Order Finite Element Methods”, Chapman & Hall/CRC, London, ISBN 1 58488 438-X

[7] Jan Pomplun, “Rigorous FEM-Simulation of Maxwell’s Equations for EUV-Lithography" (Diplomarbeit), Konrad Zuse Institut, 2006

[8] Ronald Rook, “Notes on solving Maxwell equations Part 2: Green’s function for stratified media”, CASA report 10-??

PREVIOUS PUBLICATIONS IN THIS SERIES:

Number	Author(s)	Title	Month
11-06	M.E. Hochstenbach L. Reichel	Fractional Tikhonov regularization for linear discrete ill-posed problems	Jan. '11
11-07	W. Hoitinga E.H. van Brummelen	A discontinuous Galerkin finite-element method for a 1D prototype of the Boltzmann equation	Jan. '11
11-08	M.V. Ugryumova W.H.A. Schilders	Evaluation and comparison of FEM and BEM for extraction of homogeneous substrates	Febr. '11
11-09	M.V. Ugryumova W.H.A. Schilders	Efficient simulation of power MOS transistors	Febr. '11
11-10	R. Rook	Notes on solving Maxwell equations Part 1: Finite elements method using vector elements	Febr. '11

Ontwerp: de Tantes,
Tobias Baanders, CWI